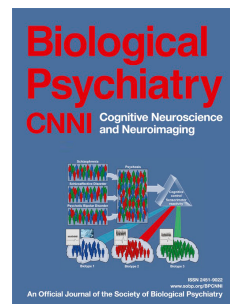


Journal Pre-proof

Resting state changes in aging and Parkinson's disease are shaped by underlying neurotransmission – a normative modeling study

Jan Kasper, Svenja Caspers, Leon D. Lotter, Felix Hoffstaedter, Simon B. Eickhoff, Juergen Dukart



PII: S2451-9022(24)00112-5

DOI: <https://doi.org/10.1016/j.bpsc.2024.04.010>

Reference: BPSC 1215

To appear in: *Biological Psychiatry: Cognitive Neuroscience and Neuroimaging*

Received Date: 14 January 2024

Revised Date: 15 March 2024

Accepted Date: 16 April 2024

Please cite this article as: Kasper J., Caspers S., Lotter L.D., Hoffstaedter F., Eickhoff S.B. & Dukart J., Resting state changes in aging and Parkinson's disease are shaped by underlying neurotransmission – a normative modeling study, *Biological Psychiatry: Cognitive Neuroscience and Neuroimaging* (2024), doi: <https://doi.org/10.1016/j.bpsc.2024.04.010>.

This is a PDF file of an article that has undergone enhancements after acceptance, such as the addition of a cover page and metadata, and formatting for readability, but it is not yet the definitive version of record. This version will undergo additional copyediting, typesetting and review before it is published in its final form, but we are providing this version to give early visibility of the article. Please note that, during the production process, errors may be discovered which could affect the content, and all legal disclaimers that apply to the journal pertain.

© 2024 Society of Biological Psychiatry. Published by Elsevier Inc. All rights reserved.

Resting state changes in aging and Parkinson's disease are shaped by underlying neurotransmission – a normative modeling study

Jan Kasper^{1,2}, Svenja Caspers^{3,4}, Leon D. Lotter^{1,2,5}, Felix Hoffstaedter^{1,2}, Simon B. Eickhoff^{1,2}, Juergen Dukart^{1,2,*}

¹Institute of Systems Neuroscience, Medical Faculty and University Hospital Düsseldorf, Heinrich Heine University Düsseldorf, Düsseldorf, Germany

²Institute of Neuroscience and Medicine (INM-7), Research Centre Jülich, Jülich, Germany

³Institute for Anatomy I, Medical Faculty and University Hospital Düsseldorf, Heinrich Heine University Düsseldorf, Düsseldorf, Germany

⁴Institute of Neuroscience and Medicine (INM-1), Research Centre Jülich, Jülich, Germany

⁵Max Planck School of Cognition, Stephanstrasse 1A, 04103 Leipzig, Germany

***Corresponding author:**

Juergen Dukart, PhD

Institute of Systems Neuroscience, Medical Faculty, Heinrich Heine University Düsseldorf

Institute of Neuroscience and Medicine - INM-7: Brain and Behaviour, Research Center Jülich

Wilhelm-Johnen-Straße,

52425 Jülich, Germany

Email: j.dukart@fz-juelich.de

Running title: Co-localization of brain function and neurotransmitters

Keywords: Aging; Resting-state fMRI; PET; Neurotransmitter systems; Parkinson's disease; Normative modeling

Abstract

Background

Human healthy and pathological aging is linked to a steady decline in brain resting state activity and connectivity measures. The neurophysiological mechanisms underlying these changes remain poorly understood.

Methods

Making use of recent developments in normative modeling and availability of *in vivo* maps for various neurochemical systems, we test in the UK Biobank cohort ($N=25917$) if and how age- and Parkinson's disease related resting state changes in commonly applied local and global activity and connectivity measures co-localize with underlying neurotransmitter systems.

Results

We find the distributions of several major neurotransmitter systems including serotonergic, dopaminergic, noradrenergic, and glutamatergic neurotransmission to correlate with age-related changes as observed across functional activity and connectivity measures. Co-localization patterns in Parkinson's disease deviate from normative aging trajectories for these, as well as for cholinergic and GABAergic, neurotransmission. The deviation from normal co-localization of brain function and GABAa correlates with disease duration.

Conclusions

These findings provide new insights into molecular mechanisms underlying age- and Parkinson's related brain functional changes by extending the existing evidence elucidating

the vulnerability of specific neurochemical attributes to normal aging and Parkinson's disease. The results particularly indicate that alongside dopamine and serotonin, increased vulnerability of glutamatergic, cholinergic, and GABAergic systems may also contribute to Parkinson's disease-related functional alterations. Combining normative modeling and neurotransmitter mapping may aid future research and drug development through deeper understanding of neurophysiological mechanisms underlying specific clinical conditions.

Introduction

Understanding neurophysiological mechanisms underlying healthy and pathological brain aging is essential for successful prevention, detection, and intervention strategies against age-related diseases and cognitive decline. Despite ample evidence for age-related decline in various brain functional measures, understanding of the neurophysiological mechanisms underlying these changes is limited. As the interplay of different neurotransmitter systems contributes substantially to the blood oxygen level dependent (BOLD) signal, changes in these systems likely contribute to age-related functional alterations as observed using resting state functional magnetic resonance imaging (rs-fMRI).

Most commonly applied rs-fMRI measures estimate either local activity or synchronicity by assessing temporal changes in regional BOLD amplitude or BOLD signal correlation across regions. Previous rs-fMRI studies reported aging-related reductions in local brain activity primarily in medial and frontal regions(1–4). These alterations are complemented by reduced local synchronicity in cortical, sub-cortical, and cerebellar motor structures(5) and increased local synchronicity mainly in hippocampal and thalamic regions(4,6). Positron emission tomography (PET) studies of aging reported reduced serotonergic(7–11), dopaminergic(12–15), glutamatergic(16–18), cholinergic(19), and norepinephrinergic(20) neurotransmission and increased availability of GABAa(21) and μ -opioid(22) receptors. Whilst both modalities point to complex functional re-organization during aging, the relationship between the respective rs-fMRI and PET findings remains poorly understood.

Studying associations between PET-derived regional receptor or transporter availability and rs-fMRI-derived functional signal has been shown to be a promising way to estimate their impact on the observed brain phenotypes(23,24). Yet, age-related changes in these associations have not been systematically addressed. These changes may reflect altered

availability or functional decline of cell populations with corresponding neurochemical properties. Following this logic, disease related changes in such associations would support the notion of respective neurotransmitter systems being particularly affected by the respective neuropathology(25).

Understanding of typical age-related co-localization changes of brain function and neurotransmitter systems can inform the study of pathological deviations from such as for example observed in Parkinson's disease(25) (PD). Normative models, as recently applied to MRI data(26–28), may prove suitable for characterizing such spatial co-localizations. Such models allow individual participants or patients to be compared with the typical trajectories derived from large representative populations by incorporating non-constant percentiles of variation and also variation within the cohort of interest(29).

Previous studies provided evidence for increased vulnerability of specific neurotransmitter systems in PD including dopaminergic(30–35), serotonergic(36–38), glutamatergic(39,40), GABAergic(34), histaminergic(41), cholinergic(42–44), and norepinephrinergic(45,46) neurotransmission. In our previous work, functional alterations in PD were related to the availability of D2 and 5-HT1b receptors, supporting the notion of specific vulnerability of these neurotransmitter systems(25). However, if and how far these PD-related alterations deviate from typical age-related co-localization changes remains to be shown.

To address these questions, we adopt a normative modeling approach to test for aging effects on co-localizations between brain functional measures and underlying neurotransmission in the UK Biobank cohort. We test for co-localization of PET-derived distributions for major neurotransmitter systems with commonly deployed rs-fMRI-derived activity and connectivity measures during aging and in PD.

Methods

Cohorts

We included 25917 adult subjects from the UK Biobank not diagnosed with psychiatric, cognitive, and neurological disorders (Supplementary Table 1) with known effect on brain structure and function as a control cohort. We additionally identified a group of 58 subjects from the UK Biobank who were diagnosed with idiopathic Parkinson's disease (ICD-10, G20) before their imaging session. An overview of both groups is provided in Table 1.

Processing of resting state functional imaging data

We used resting state functional MRI data from the UK Biobank, initially processed according to their documentation(47). We normalized (MNI space), smoothed, and bandpass-filtered these images to enhance the signal-to-noise ratio of neuronal activity in the BOLD signal. Control measures were implemented to mitigate confounding effects of motion, white matter, and cerebrospinal fluid. Data quality was further improved by discarding images exhibiting distortions and artifacts, including those attributed to within-scanner motion. Details on preprocessing procedures, metrics calculation, and key figures for data analysis are provided in the Supplementary Methods.

Three complementary voxel-wise maps of brain function, including measures of neuronal activity and synchronicity were derived from individual, preprocessed rs-fMRI data. Fractional amplitude of low-frequency fluctuations (fALFF(48)) was computed as the power ratio of neuronal activity-related oscillations to the total detectable frequency range in the

BOLD signal. Local correlation (LCOR(49)) and global correlation (GCOR(50)) characterized BOLD similarity, reflecting the voxel's correlation either with its local vicinity or with all other voxels, respectively.

Aging effects and sex differences in fALFF, LCOR, and GCOR

Both, voxel-wise aging effects and sex differences were estimated by general linear modeling of (t-)contrast maps using a family-wise-error corrected voxel-wise threshold of $P<0.05$ combined with a cluster-defining threshold of $k>20$ including sex or age and total intracranial volume (TIV) as covariates, respectively. Maps of annual changes in fALFF, LCOR, and GCOR were generated from voxel-wise beta weights.

Spatial co-localization of brain function and neurotransmitter systems and effects of aging in the healthy population

We analyzed to what extent unthresholded group-level aging effects (maps of annual change) in fALFF, LCOR, and GCOR co-localize with specific neurotransmitter systems. Spearman correlation coefficients were derived using the default Neuromorphometrics atlas (119 regions) estimating the similarity of aging effects in fALFF, LCOR, and GCOR with 19 distinct neurotransmitter maps as included in the JuSpace toolbox(25). To approximate a normal distribution, correlation coefficients were Fisher's z-transformed. As shown in our previous study(51), the choice of atlas (with a comparable number of parcels) has a neglectable effect on the observed co-localization patterns. This atlas was used as it provides a neuroanatomically plausible delineation of cortical and subcortical structures.

Included PET maps were derived from independent healthy volunteer populations and covered serotonergic receptors (5-HT_{1a}(52), 5-HT_{1b}(53), 5-HT_{2a}(52), 5-HT₄(52), 5-HT₆(11)), dopaminergic receptors (D₁(54), D₂(55)), histamine receptor 3 (H₃(56)), dopamine uptake (DAT(24)), serotonin (SERT(52)), norepinephrine (NET(20)), vesicular acetylcholine (VACHT(57)) transporters, cholinergic receptors (M₁(58), A_{4B2}(59)), glutamate receptors (mGluR₅(60), NMDA(61)), cannabinoid CB₁(62), opioid μ (57), and the GABA_A(24) receptor. Source publications and sample characteristics of each PET map are provided in Supplementary Table 2. 95% confidence intervals of Spearman correlation coefficients were estimated using the Bonett-Wright(63) procedure.

We re-computed correlations with all PET maps using single-subject measures of fALFF, LCOR, and GCOR for a greater insight in how group-level aging effects are also reflected in terms of the magnitude and spread across individual data. Before testing for aging effects across individual co-localizations, we examined whether Fisher's z-transformed Spearman correlation coefficients of the healthy population differed significantly from a null distribution (one-sample t-test, alpha=0.05). Aging effects on co-localization strengths were then estimated using linear regression analyses considering sex as a confound.

Higher variation in co-localization between brain function and neurotransmitter systems with aging

Distinct aging trajectories from healthy aging to the effects of diseases and impairments are known to manifest in altered brain function. Depending on the underlying neurophysiological processes functional changes are likely to be architecturally aligned with the spatial patterns of affected neurotransmitter systems. Correspondingly, one would expect to observe an increased variance in co-localizations in older as compared to younger participants. To test

this hypothesis, we examined the heteroscedasticity to identify neurotransmitter systems affected by such age-related brain functional changes in two steps.

Using the White test, we first identified all pairs of brain function measures and PET maps whose correlation coefficients exhibit non-constant variance across age. In a post-hoc analysis, we tested for each co-localization pair with non-constant variance ($P_{FDR}<0.05$) whether the variance for individuals in the upper third age-range is higher as compared to those in the lower third age-range using the Goldfeld-Quandt-test (one-sided, i.e., increasing variance). We regressed out sex effects prior to the comparisons.

Normative modeling of brain function - neurotransmitter co-localization and deviations in Parkinson's disease

To model aging effects on the observed co-localization patterns, we generated normative models based on the Fisher's transformed correlation coefficients derived from the healthy subjects using the PCNtoolkit(64) (cf. Supplementary Methods for more details on model construction and Figure 1 for a methodological overview).

For subjects with PD, deviations (z-scores) from these normative aging models were derived per neurotransmitter map. For each model, we examined whether the PD deviation scores were significantly different from a null distribution (t-test, alpha=0.05) and whether they were correlated with disease duration and cognitive scores (details are provided in Supplementary Tables 23-29). In addition, we wanted to know which brain regions contributed most to significant deviations ($P_{FDR}<0.05$) and whether functional differences to a normal sub-population explain these regional contributions. To this end, we repeated the co-localization analysis in the data of PD using a leave-one-region-out approach(65) to obtain maps of regional contribution ($\Delta\rho^2$) to the deviation. Further, we calculated regional functional

differences (Cohen's d) in fALFF, LCOR, and GCOR in PD compared to an age- and sex-matched healthy subgroup (n=17400).

All analyses were corrected for multiple comparisons using either the Benjamini-Hochberg procedure or, in case of inflated P-values due to large sample sizes, Bonferroni-Holm correction. Additionally, to minimize the influence of underlying atrophy on co-localization changes, we repeated all analyses after regressing out individual voxel-wise grey matter volumes from all functional maps.

Results

Demographic characterization

From a total pool of 30035 subjects from the UK Biobank for which all necessary data was available, our analysis was based on data of 25917 subjects for whom no diseases with known effect on brain function were reported.

The analysis was repeated on 25914 subjects after accounting for age-related atrophy, excluding three subjects with structural data. 75 subjects of the total pool had reported a diagnosis of Parkinson's disease. 58 of them were classified as "manifest" because their first report of PD was dated before their imaging session. In order to compare regional measures of brain function in PD with those of the healthy controls, we defined an age- and sex-matched subcohort consisting of 17400 subjects (PD mean \pm SD age in years: 68.6 ± 6.5 , HC_{matched} mean \pm SD age: 67.6 ± 6.0 , P>0.26; 55.17% male PD and 51.7% male HC_{matched}, $\chi^2(1)=0.29$, P=0.59). An overview of the groups is provided in Table 1.

Group-level aging effects in resting state measures and their co-localization to underlying neurotransmission

All three functional measures decreased with aging in most cortical, sub-cortical, and cerebellar regions. Each measure showed a wide-spread but distinct spatial pattern of age-related alterations with few regional increases (Figure 2A, Supplementary Table 3 and Supplementary Table 4).

Next, we aimed to understand if the topography of age-related changes correlated with distributions of specific neurotransmitter systems. For this, we derived voxel-wise maps of age-related annual changes in all three measures and examined their spatial co-localization with the neurotransmitter systems. Annual changes in fALFF and LCOR correlated significantly ($P_{FDR}<0.05$) with serotonergic, dopaminergic, norepinephrinergic (also GCOR) and glutamate neurotransmission (Figure 2B, Supplementary Figures 1–2, Supplementary Tables 5–6). fALFF and LCOR changes correlated with GABAergic cholinergic neurotransmission, respectively. Except for the correlation between fALFF changes and NMDA all findings remained significant after correcting for age-related atrophy. Scatter plots of the strongest correlations are displayed in Figure 2B. Results for voxel-wise sex differences are summarized in Supplementary Figures 3–5 and Supplementary Tables 7–10.

Individual co-localization of resting state measures and neurotransmitter systems covaries with age

The extent to which a specific neurotransmitter system contributes to the measured brain function was evaluated by its correlation strength. We first computed individual co-localization strengths between each subject's resting-state measure and each neurotransmitter

map. Due to the large cohort size, even very small effects in all functional measures were significantly associated with the 19 PET maps (all $P_{\text{Bonferroni-Holm}} < 0.001$, median absolute Spearman correlation coefficient ranged from 0.03 to 0.68) with different neurotransmitter systems explaining between 0.1% and 46% of variance in the respective resting state measures (Supplementary Figure 6, Supplementary Tables 11–13, left columns). The direction of the correlations was highly similar across the three measures. Positive correlations were found for the norepinephrinergic, muscarinic, glutamatergic, GABAergic systems, and serotonergic receptors 5-HT1b, -2a, and -6. Negative correlations were found for the dopaminergic, histaminergic, and opioid neurotransmitter systems, for serotonin receptors 5-HT1a and 5-HT4, and serotonin and vesicular acetylcholine transporters (SERT and VACHT). All associations remained significant after controlling for age-related atrophy (Supplementary Tables 14–16). If age-related changes in brain functions are predominantly influenced by specific neurotransmitter systems, correlation coefficients should systematically (that is, in simplest approximation, linearly) increase or decrease during aging. Thus, we evaluated whether and to what extent aging effects and their co-localizations with neurotransmitter systems observed at the cohort level are also reflected in the individual co-localization strength. Most of the observed correlations were significantly associated with age explaining up to 3%, 4% and 1% of the co-localization strength between fALFF (with NMDA and SERT), LCOR (with SERT) and GCOR (with VACHT) and the respective neurotransmitter systems (Figure 3A, Supplementary Tables 11–13, middle columns). Correction for atrophy lowered the correlation strengths for most associations but the findings remained largely significant (Supplementary Tables 14–16, middle columns).

Variance in co-localization changes during aging

As aging might not only have affected average co-localization strengths but might also have led to increased variance (i.e., due to yet undetected neurodegenerative processes in a subpopulation) we tested for such changes using a two-step procedure. Using the White-test, we identified significant non-constant variance in co-localization strength. For fALFF and LCOR, non-constant variance was observed for all neurotransmitter classes, except for LCOR and the opioid system. For GCOR, significant non-constant variance in co-localization was found for serotonergic, norepinephrinergic, cannabinoid, opioid, glutamatergic, and cholinergic neurotransmission (Supplementary Table 17, left columns). These effects remained significant after controlling for atrophy except for GCOR and 5-HT1b, 5-HT6, and SERT (Supplementary Table 18, left columns). As the previous analysis only detected differences in variance across age but not their direction, we proceeded to perform the Goldfeld-Quandt test. Here, we compared the co-localization variance between the youngest (44–60 years) and oldest (68–82 years) third ($n_{\text{Both}}=8639$) of the study population for the previously identified significant non-constant variances (Figure 3B).

For fALFF and LCOR, higher variability in co-localization was found in the elderly sub-population for serotonergic, dopaminergic, noradrenergic, histaminergic, cannabinoid, glutamatergic, and cholinergic neurotransmission. In addition, for LCOR, we found significantly higher variance in the older population in co-localization with the GABA system. For GCOR, higher variability in co-localization was found regarding the serotonergic, noradrenergic, glutamatergic, and cholinergic system. For fALFF, 11 out of 14, for LCOR, 14 out of 15, and for GCOR, 7 out of 11 neurotransmitter co-localization pairs, as identified using the White-test, displayed a higher variance in the older subpopulation (Figure 3B, Supplementary Table 17, right columns). The effects remained largely similar after controlling for atrophy (Supplementary Table 18, right columns).

Deviations from normal co-localization in manifest Parkinson's disease

Having established this reference for co-localization of normal age-related changes with different neurotransmitter systems, we now aimed to test if and how functional changes caused by progressive neurodegeneration deviated from the non-pathological co-localization patterns. For this, we adopted a normative modeling approach using the healthy aging population as a reference (models are visualized in Supplementary Figures 7–8). A UK Biobank subgroup of PD patients served as an example for the clinical relevance of our findings. For fALFF, PD patients had a lower co-localization strength with serotonergic, GABAergic, muscarinic, and glutamatergic neurotransmission (Figure 4D). For LCOR and GCOR, PD showed lower co-localizations with serotonergic, dopaminergic, GABAergic, histaminergic, norepinephrinergic, glutamatergic, and cholinergic neurotransmitter systems (Figure 4E–F, Supplementary Table 19). The deviation in co-localization strength regarding LCOR and GABAa (illustrated in Figure 4A–B) correlated negatively with disease duration, with higher deviations being indicative of longer disease duration (Pearson $r=-0.38$, $P_{FDR}=0.027$; Figure 4C, Supplementary Tables 21–22). No significant correlations were found between PD-related deviations in co-localization strengths and the cognitive score (cf. Supplementary Table 23–29). After atrophy correction, all deviations remained significant except for the LCOR-5-HT1b and LCOR-VACHT associations (Supplementary Table 20).

Lastly, we aimed to understand which regions contribute most to the observed co-localization alterations in PD. For fALFF, the main contributing regions to co-localization changes in PD were the basal ganglia, insula, and occipital regions. For LCOR and GCOR, main contributing regions - were the basal ganglia, subcallosal areas, thalamus (LCOR only), basal forebrain, as well as pre- and postcentral, insula, and occipital regions (Supplementary Figures 9–11). The effects remained largely similar after controlling for atrophy (Supplementary Figures 12–14).

Regional contribution to the deviations found regarding the glutamatergic system significantly correlated with regional alteration in PD in both synchronicity measures ($P_{FDR} < 0.05$, Supplementary Figures 15–16, Supplementary Tables 29–30; Figure 4G-H: Effect sizes in regions with FDR-significant differences in LCOR and GCOR in PD vs. matched HC; Tables 31–32: Regional comparison of fALFF, LCOR, and GCOR in PD vs. matched HC; Supplementary Figures 17–19: Regional effect sizes in fALFF, LCOR, and GCOR in PD vs. matched HC).

Discussion

Here, we test how age-related changes in commonly applied resting activity and connectivity measures co-localize with underlying neurotransmission. Consistent with previous studies of aging effects on brain function, we find widespread age-related decreases but also few increases in the three evaluated measures(2,3,66). These age-related changes display a robust co-localization pattern with various major neurotransmitter systems, including monoamines, glutamate, choline, and GABA, at group- and single-subject level. Variance in the co-localization patterns of these systems increases over age. PD patients display significant deviations from typical age-related co-localization patterns in neurotransmitter systems related to the disease. The deviation in co-localization strength regarding the GABAergic system correlates with disease duration.

In line with most studies reporting aging effects in the brain, we find wide-spread age-related decreases in all three evaluated functional measures(1–5). The extent of the decreases is substantially higher in our study covering basically all of the brain with few exceptions as discussed below. Considering the large cohort size, the increased statistical power as

compared to previous studies with at most few hundred participants is the most likely explanation for the observed discrepancy. In parallel, we observe spatially distinct age-related increases across the three evaluated measures covering parietal, precuneal, thalamic, gyrus rectus, and cerebellar regions. Recent theories of neurocognitive aging including dedifferentiation(67) and scaffolding (68)) may provide potential explanations for these patterns of brain functional alteration. Neuronal compensation and inefficiency may be associated with increased or decreased cognitive functioning, respectively(69,70). With respect to directionality, our findings are consistent with several previous studies, suggesting presumably compensation-related increases in different connectivity metrics in the aging population(66,71). However, such locally restricted increases aside with the observed global decreases may also be attributed to a loss of functional differentiation leading to unorganized additional activation or suppression across different regions, or to reduced neural efficiency leading to an inability to suppress specific activation patterns(69).

Supporting the previously reported complex re-organization of the excitation/inhibition balance during aging(72), we find the group-level aging effects on brain function to be associated with glutamatergic and GABAergic neurotransmission. The additional co-localization of the aging effects with monoaminergic and cholinergic systems may be supportive of the underlying changes to be related to learning, memory, and other higher cognitive functions affected by aging(7,15,71,73). In contrast, the age-related global connectivity is primarily increased in thalamic and cerebellar regions and the topography of these changes only aligns with the norepinephrinergic neurotransmission. Both regions and in particular the thalamus show a high expression of norepinephrine receptors(74,75). Whilst the modulatory role of norepinephrine in the cerebellum has been repeatedly associated with motor learning(76,77), its contribution to aging is controversially discussed with its activity being associated with prevention but also acceleration of the production and accumulation of amyloid- β and tau across the brain(78). On a functional level, these findings may be related to

the functional decline of the norepinephrine system, which is considered as key factor in maintaining arousal and cognitive adaptation and control(79)(80).

When testing for co-localization of functional measures with neurotransmission at the single subject level, we find age-related alterations in all three measures to co-localize primarily with monoaminergic neurotransmission. Increases in variance observed for a variety of evaluated neurotransmitter systems complemented these findings. Considering the reportedly high prevalence of neuropathology in a cognitively normal elderly population(81,82) the individual co-localization changes - aside with increased variance - may reflect such yet undetected neurodegenerative processes. To test the sensitivity of the co-localization patterns to such neurodegenerative processes we further adopted a normative modeling approach. A major advantage of normative models is their ability to represent population heterogeneity in the phenotype under investigation by means of normalized deviation scores(64). We applied this approach in patients with a diagnosis of PD, which was previously linked to monoaminergic neurotransmission as well as more recently to a dysbalance of GABA and glutamate(83–85). Indeed, in PD patients, co-localization patterns significantly deviate from age- and sex-adjusted normative models across various neurotransmitter systems and all three functional metrics. Deviations in local activity co-localization are found primarily with respect to serotonergic, GABA, and glutamatergic neurotransmission, whilst deviations in co-localization of both connectivity measures are also present with respect to dopamine neurotransmission. We find that only the deviation in co-localization strength of local connectivity with GABAa receptors predicts disease duration supporting the suggested relevance of GABA pathology for clinical progression(83).The observed age-related increases in variance regarding GABAergic co-localization with brain function supports the notion of its contribution to potential pathophysiological changes in parts of the aging populations. This interpretation is also supported by its association with disease duration in PD patients in our study. In line with that, GABAergic system changes have recently been reported in PD and

were associated with visual hallucinations and axial symptoms (such as postural instability, rigidity and bradykinesia)(86–88). The observed distinct co-localization patterns of various neurotransmitter systems with functional changes in aging and PD point to distinct pathophysiological processes affecting the respective processes. Such insights, if confirmed by other modalities, may aid identification of novel drug targets as well as aid development of successful monitoring strategies for the respective pathophysiological changes.

The studied cohort was recruited as a representative sample of healthy UK residents. Because the metrics target local brain function, subjects with diseases primarily affecting brain structure or function were excluded. Given the prevalence for mild depressive symptoms of the UK population of 11%(89) and that 12.32% of our analyzed participants of the UK Biobank have a reference to ICD-10: F32, their exclusion would have biased the cohort. PD appearance and progression is highly heterogeneous. As no scores for PD severity (i.e. Unified Parkinson's Disease Rating Scale(90) or Hoehn & Yahr stages(91)) and only a limited number of cognitive scores were available, we could only roughly approximate PD severity based on disease duration. As PD medication is known to affect measures of brain function, it may have contributed to some of the effects observed in the PD cohort in our study. However, the effects of PD medication on spatial co-localization have been previously shown to be rather negligible as compared to the effects of PD(25). Additional healthy control biases in the UK biobank(92) include a high average socioeconomic status and low alcohol and tobacco consume. Although the socio-economic status may be associated with cognitive reserve through strengthened cognitive abilities during childhood(93,94), we estimate that deviations from the overall population results are small with respect to these primary biases. Further sampling of a more diverse population is needed to address the potential impact of such biases. Clinical scores of disease severity should be used to strengthen evidence of the observed association with GABAergic neurotransmission. Using PET maps from differently

aged healthy populations may introduce a further bias into our findings as proteomics such as receptor and transporter distributions may change during aging(79,95).

Conclusions

Here, we provided a detailed overview on aging effects on macroscopic brain functioning as observed using common rs-fMRI-derived measures of local activity and local and global connectivity. We link these age-related changes to the distribution of various neurotransmitter systems demonstrating a decline in co-localization strength aside with increased variance during aging. By adopting a normative modeling approach on the example of PD, we further demonstrate the feasibility of using co-localization strength as a sensitive measure of neurodegeneration, providing potentially valuable insight into the underlying neuropathological processes.

Declaration of Interests

The authors report no biomedical financial interests or potential conflicts of interest.

Acknowledgements

The authors are grateful for the immense work of the whole UK Biobank team, as well as all the volunteers who contributed to this dataset of inestimable value. JD has received funding

from the European Union's Horizon 2020 research and innovation program under grant agreement No. 826421, "TheVirtualBrain-Cloud". SC and SBE have received funding from the European Union's Horizon 2020 research and innovation program under grant agreement No. 945539 (Human Brain Project SGA3). LDL was supported by the Federal Ministry of Education and Research (BMBF) and the Max Planck Society (MPG), Germany.

References

1. Biswal BB, Mennes M, Zuo X-N, Gohel S, Kelly C, Smith SM, et al. (2010): Toward discovery science of human brain function. *Proc Natl Acad Sci USA* 107: 4734–4739.
2. Hu S, Chao HH-A, Zhang S, Ide JS, Li C-SR (2014): Changes in cerebral morphometry and amplitude of low-frequency fluctuations of BOLD signals during healthy aging: correlation with inhibitory control. *Brain Struct Funct* 219: 983–994.
3. Vieira BH, Rondinoni C, Garrido Salmon CE (2020): Evidence of regional associations between age-related inter-individual differences in resting-state functional connectivity and cortical thinning revealed through a multi-level analysis. *NeuroImage* 211: 116662.
4. Montalà-Flaquer M, Cañete-Massé C, Vaqué-Alcázar L, Bartrés-Faz D, Peró-Cebollero M, Guàrdia-Olmos J (2023): Spontaneous brain activity in healthy aging: An overview through fluctuations and regional homogeneity. *Front Aging Neurosci* 14: 1002811.
5. Wu T, Zang Y, Wang L, Long X, Li K, Chan P (2007): Normal aging decreases regional homogeneity of the motor areas in the resting state. *Neuroscience Letters* 423: 189–193.
6. Harrison TM, Maass A, Adams JN, Du R, Baker SL, Jagust WJ (2019): Tau deposition is associated with functional isolation of the hippocampus in aging. *Nat Commun* 10: 4900.

7. Karrer TM, McLaughlin CL, Guaglianone CP, Samanez-Larkin GR (2019): Reduced serotonin receptors and transporters in normal aging adults: a meta-analysis of PET and SPECT imaging studies. *Neurobiology of Aging* 80: 1–10.
8. Sheline YI, Mintun MA, Moerlein SM, Snyder AZ (2002): Greater Loss of 5-HT_{2A} Receptors in Midlife Than in Late Life. *AJP* 159: 430–435.
9. Nord M, Cselenyi Z, Forsberg A, Rosenqvist G, Tiger M, Lundberg J, et al. (2014): Distinct regional age effects on [¹¹C]AZ10419369 binding to 5-HT 1B receptors in the human brain. *NeuroImage* 103: 303–308.
10. Madsen K, Haahr MT, Marner L, Keller SH, Baaré WF, Svarer C, et al. (2011): Age and sex effects on 5-HT₄ receptors in the human brain: A [¹¹C]SB207145 PET study. *J Cereb Blood Flow Metab* 31: 1475–1481.
11. Radhakrishnan R, Nabulsi N, Gaiser E, Gallezot J-D, Henry S, Planeta B, et al. (2018): Age-Related Change in 5-HT₆ Receptor Availability in Healthy Male Volunteers Measured with ¹¹C-GSK215083 PET. *J Nucl Med* 59: 1445–1450.
12. Antonini A, Leenders KL, Reist H, Thomann R, Beer H-F, Locher J (1993): Effect of Age on D2 Dopamine Receptors in Normal Human Brain Measured by Positron Emission Tomography and ¹¹C-Raclopride. *Archives of Neurology* 50: 474–480.
13. Seaman KL, Smith CT, Juarez EJ, Dang LC, Castrellon JJ, Burgess LL, et al. (2019): Differential regional decline in dopamine receptor availability across adulthood: Linear and nonlinear effects of age. *Hum Brain Mapp* hbm.24585.
14. Wang Y, Chan GLY, Holden JE, Dobko T, Mak E, Schulzer M, et al. (1998): Age-dependent decline of dopamine D1 receptors in human brain: A PET study. *Synapse* 30: 56–61.
15. Karrer TM, Josef AK, Mata R, Morris ED, Samanez-Larkin GR (2017): Reduced dopamine receptors and transporters but not synthesis capacity in normal aging adults: a meta-analysis. *Neurobiology of Aging* 57: 36–46.
16. Magnusson (2010): Selective vulnerabilities of N-methyl-D-aspartate (NMDA) receptors during brain aging. *FrontiAgNeurosci*. <https://doi.org/10.3389/fnagi.2010.00011>

17. Perry EK, Piggott MA, Court JA, Johnson M, Perry RH (1993): Transmitters in the Developing and Senescent Human Brain. *Annals of the New York Academy of Sciences* 695: 69–72.
18. Piggott MA, Perry EK, Perry RH, Court JA (1992): [3H]MK-801 binding to the NMDA receptor complex, and its modulation in human frontal cortex during development and aging. *Brain Research* 588: 277–286.
19. Zubieta J-K, Koepp RA, Frey KA, Kilbourn MR, Mangner TJ, Foster NL, Kuhl DE (2001): Assessment of muscarinic receptor concentrations in aging and Alzheimer disease with [11C]NMPB and PET. *Synapse* 39: 275–287.
20. Ding Y-S, Singhal T, Planeta-Wilson B, Gallezot J-D, Nabulsi N, Labaree D, et al. (2010): PET imaging of the effects of age and cocaine on the norepinephrine transporter in the human brain using (S,S)-[¹¹C]O-methylreboxetine and HRRT. *Synapse* 64: 30–38.
21. Cuypers K, Hehl M, Van Aalst J, Chalavi S, Mikkelsen M, Van Laere K, et al. (2021): Age-related GABAergic differences in the primary sensorimotor cortex: A multimodal approach combining PET, MRS and TMS. *NeuroImage* 226: 117536.
22. Zubieta J-K, Dannals RF, Frost JJ (1999): Gender and Age Influences on Human Brain Mu-Opioid Receptor Binding Measured by PET. *AJP* 156: 842–848.
23. Hansen JY, Shafiei G, Markello RD, Smart K, Cox SML, Nørgaard M, et al. (2022): Mapping neurotransmitter systems to the structural and functional organization of the human neocortex. *Nat Neurosci* 25: 1569–1581.
24. Dukart J, Holiga Š, Chatham C, Hawkins P, Forsyth A, McMillan R, et al. (2018): Cerebral blood flow predicts differential neurotransmitter activity. *Sci Rep* 8: 4074.
25. Dukart J, Holiga S, Rullmann M, Lanzenberger R, Hawkins PCT, Mehta MA, et al. (2021): JuSpace: A tool for spatial correlation analyses of magnetic resonance imaging data with nuclear imaging derived neurotransmitter maps. *Hum Brain Mapp* 42: 555–566.
26. Marquand AF, Haak KV, Beckmann CF (2017): Functional corticostriatal connection topographies predict goal-directed behaviour in humans. *Nat Hum Behav* 1: 0146.

27. Wolfers T, Beckmann CF, Hoogman M, Buitelaar JK, Franke B, Marquand AF (2020): Individual differences v. the average patient: mapping the heterogeneity in ADHD using normative models. *Psychol Med* 50: 314–323.
28. Fraza CJ, Dinga R, Beckmann CF, Marquand AF (2021): Warped Bayesian linear regression for normative modelling of big data. *NeuroImage* 245: 118715.
29. Ziegler G, Ridgway GR, Dahnke R, Gaser C (2014): Individualized Gaussian process-based prediction and detection of local and global gray matter abnormalities in elderly subjects. *NeuroImage* 97: 333–348.
30. Kaasinen V, Vahlberg T, Stoessl AJ, Strafella AP, Antonini A (2021): Dopamine Receptors in Parkinson's Disease: A Meta-Analysis of Imaging Studies. *Mov Disord* 36: 1781–1791.
31. Kaasinen V, Nagren K, Hietala J, Oikonen V, Vilkman H, Farde L, et al. (2000): Extrastriatal dopamine D2 and D3 receptors in early and advanced Parkinson's disease. *Neurology* 54: 1482–1487.
32. Seeman P, Niznik HB (1990): Dopamine receptors and transporters in Parkinson's disease and schizophrenia. *FASEB j* 4: 2737–2744.
33. Politis M, Piccini P, Pavese N, Koh S-B, Brooks DJ (2008): Evidence of dopamine dysfunction in the hypothalamus of patients with Parkinson's disease: An in vivo 11C-raclopride PET study. *Experimental Neurology* 214: 112–116.
34. Takashima H, Terada T, Bunai T, Matsudaira T, Obi T, Ouchi Y (2022): In vivo Illustration of Altered Dopaminergic and GABAergic Systems in Early Parkinson's Disease. *Front Neurol* 13: 880407.
35. Yao N-T, Zheng Q, Xu Z-Q, Yin J-H, Lu L-G, Zuo Q, et al. (2020): Positron emission computed tomography/single photon emission computed tomography in Parkinson disease. *Chinese Medical Journal* 133: 1448–1455.
36. Huot P, Fox SH, Brotchie JM (2011): The serotonergic system in Parkinson's disease. *Progress in Neurobiology* 95: 163–212.

37. Melse M, Tan SKH, Temel Y, van Kroonenburgh MJPG, Leentjens AFG (2014): Changes in 5-HT2A Receptor Expression in Untreated, de novo Patients with Parkinson's Disease. *Journal of Parkinson's Disease* 4: 283–287.
38. Varrone A, Svenningsson P, Forsberg A, Varnäs K, Tiger M, Nakao R, et al. (2014): Positron emission tomography imaging of 5-hydroxytryptamine1B receptors in Parkinson's disease. *Neurobiology of Aging* 35: 867–875.
39. Kang Y, Henchcliffe C, Verma A, Vallabhajosula S, He B, Kothari PJ, et al. (2019): 18F-FPEB PET/CT Shows mGluR5 Upregulation in Parkinson's Disease: mGluR5 and DaT in PD. *Journal of Neuroimaging* 29: 97–103.
40. Zhang Z, Zhang S, Fu P, Zhang Z, Lin K, Ko JK-S, Yung KK-L (2019): Roles of Glutamate Receptors in Parkinson's Disease. *IJMS* 20: 4391.
41. Sharma A, Muresanu DF, Patnaik R, Menon PK, Tian ZR, Sahib S, et al. (2021): Histamine H3 and H4 receptors modulate Parkinson's disease induced brain pathology. Neuroprotective effects of nanowired BF-2649 and clobenpropit with anti-histamine-antibody therapy. *Progress in Brain Research*, vol. 266. Elsevier, pp 1–73.
42. Meyer PM, Tiepolt S, Barthel H, Hesse S, Sabri O (2014): Radioligand imaging of $\alpha 4\beta 2^*$ nicotinic acetylcholine receptors in Alzheimer's disease and Parkinson's disease. *Q J Nucl Med Mol Imaging* 58: 376–386.
43. Asahina M, Suhara T, Shinotoh H, Inoue O, Suzuki K, Hattori T (1998): Brain muscarinic receptors in progressive supranuclear palsy and Parkinson's disease: a positron emission tomographic study. *Journal of Neurology, Neurosurgery & Psychiatry* 65: 155–163.
44. van der Zee S, Kanel P, Gerritsen MJJ, Boertien JM, Slomp AC, Müller MLTM, et al. (2022): Altered Cholinergic Innervation in De Novo Parkinson's Disease with and Without Cognitive Impairment. *Movement Disorders* 37: 713–723.
45. Nahimi A, Kinnerup MB, Sommerauer M, Gjedde A, Borghammer P (2018): Molecular Imaging of the Noradrenergic System in Idiopathic Parkinson's Disease. *International Review of Neurobiology*, vol. 141. Elsevier, pp 251–274.

46. Brumberg J, Tran-Gia J, Lapa C, Isaias IU, Samnick S (2019): PET imaging of noradrenaline transporters in Parkinson's disease: focus on scan time. *Ann Nucl Med* 33: 69–77.
47. Smith SM, Alfaro-Almagro F, Miller KL (2020, December): UK Biobank Brain Imaging Documentation (Version 1.8). Retrieved February 13, 2023, from https://biobank.ctsu.ox.ac.uk/crystal/crystal/docs/brain_mri.pdf
48. Zou Q-H, Zhu C-Z, Yang Y, Zuo X-N, Long X-Y, Cao Q-J, et al. (2008): An improved approach to detection of amplitude of low-frequency fluctuation (ALFF) for resting-state fMRI: Fractional ALFF. *Journal of Neuroscience Methods* 172: 137–141.
49. Deshpande G, LaConte S, Peltier S, Hu X (2009): Integrated local correlation: A new measure of local coherence in fMRI data. *Hum Brain Mapp* 30: 13–23.
50. Saad ZS, Reynolds RC, Jo HJ, Gotts SJ, Chen G, Martin A, Cox RW (2013): Correcting Brain-Wide Correlation Differences in Resting-State FMRI. *Brain Connectivity* 3: 339–352.
51. Kasper J, Eickhoff SB, Caspers S, Peter J, Dogan I, Wolf RC, et al. (2023): Local synchronicity in dopamine-rich caudate nucleus influences Huntington's disease motor phenotype. *Brain* 146: 3319–3330.
52. Beliveau V, Ganz M, Feng L, Ozenne B, Højgaard L, Fisher PM, et al. (2017): A High-Resolution *In Vivo* Atlas of the Human Brain's Serotonin System. *J Neurosci* 37: 120–128.
53. Gallezot J-D, Nabulsi N, Neumeister A, Planeta-Wilson B, Williams WA, Singhal T, et al. (2010): Kinetic Modeling of the Serotonin 5-HT_{1B} Receptor Radioligand [¹¹C]P943 in Humans. *J Cereb Blood Flow Metab* 30: 196–210.
54. Kaller S, Rullmann M, Patt M, Becker G-A, Luthardt J, Girbhardt J, et al. (2017): Test–retest measurements of dopamine D1-type receptors using simultaneous PET/MRI imaging. *Eur J Nucl Med Mol Imaging* 44: 1025–1032.
55. Sandiego CM, Gallezot J-D, Lim K, Ropchan J, Lin S, Gao H, et al. (2015): Reference Region Modeling Approaches for Amphetamine Challenge Studies with [¹¹C]FLB 457 and PET. *J Cereb Blood Flow Metab* 35: 623–629.

56. Gallezot J-D, Planeta B, Nabulsi N, Palumbo D, Li X, Liu J, *et al.* (2017): Determination of receptor occupancy in the presence of mass dose: [¹¹C]GSK189254 PET imaging of histamine H₃ receptor occupancy by PF-03654746. *J Cereb Blood Flow Metab* 37: 1095–1107.
57. Aghourian M, Legault-Denis C, Soucy J-P, Rosa-Neto P, Gauthier S, Kostikov A, *et al.* (2017): Quantification of brain cholinergic denervation in Alzheimer's disease using PET imaging with [18F]-FEOBV. *Mol Psychiatry* 22: 1531–1538.
58. Naganawa M, Nabulsi N, Henry S, Matuskey D, Lin S-F, Slieker L, *et al.* (2021): First-in-Human Assessment of ¹¹C-LSN3172176, an M1 Muscarinic Acetylcholine Receptor PET Radiotracer. *J Nucl Med* 62: 553–560.
59. Hillmer AT, Esterlis I, Gallezot JD, Bois F, Zheng MQ, Nabulsi N, *et al.* (2016): Imaging of cerebral α4β2* nicotinic acetylcholine receptors with (–)-[18F]Flubatine PET: Implementation of bolus plus constant infusion and sensitivity to acetylcholine in human brain. *NeuroImage* 141: 71–80.
60. Smart K, Cox SML, Scala SG, Tippler M, Jaworska N, Boivin M, *et al.* (2019): Sex differences in [11C]ABP688 binding: a positron emission tomography study of mGlu5 receptors. *Eur J Nucl Med Mol Imaging* 46: 1179–1183.
61. Galovic M, Al-Diwani A, Vivekananda U, Torrealdea F, Erlandsson K, Fryer TD, *et al.* (2021): In Vivo NMDA Receptor Function in People with NMDA Receptor Antibody Encephalitis. *Neurology*. <https://doi.org/10.1101/2021.12.04.21267226>
62. Normandin MD, Zheng M-Q, Lin K-S, Mason NS, Lin S-F, Ropchan J, *et al.* (2015): Imaging the Cannabinoid CB1 Receptor in Humans with [¹¹C] OMAR: Assessment of Kinetic Analysis Methods, Test–Retest Reproducibility, and Gender Differences. *J Cereb Blood Flow Metab* 35: 1313–1322.
63. Bonett DG, Wright TA (2000): Sample size requirements for estimating pearson, kendall and spearman correlations. *Psychometrika* 65: 23–28.
64. Rutherford S, Kia SM, Wolfers T, Fraza C, Zabihi M, Dinga R, *et al.* (2022): The normative modeling framework for computational psychiatry. *Nat Protoc* 17: 1711–1734.

65. Lotter LD, Saberi A, Hansen JY, Misic B, Barker GJ, Bokde ALW, *et al.* (2023): *Human Cortex Development Is Shaped by Molecular and Cellular Brain Systems*. *Neuroscience*.
<https://doi.org/10.1101/2023.05.05.539537>
66. Vij SG, Nomi JS, Dajani DR, Uddin LQ (2018): Evolution of spatial and temporal features of functional brain networks across the lifespan. *NeuroImage* 173: 498–508.
67. Koen JD, Rugg MD (2019): Neural Dedifferentiation in the Aging Brain. *Trends in Cognitive Sciences* 23: 547–559.
68. Reuter-Lorenz PA, Park DC (2014): How Does it STAC Up? Revisiting the Scaffolding Theory of Aging and Cognition. *Neuropsychol Rev* 24: 355–370.
69. McDonough IM, Nolin SA, Visscher KM (2022): 25 years of neurocognitive aging theories: What have we learned? *Front Aging Neurosci* 14: 1002096.
70. Bunzeck N, Steiger TK, Krämer UM, Luedtke K, Marshall L, Obleser J, Tune S (2024): Trajectories and contributing factors of neural compensation in healthy and pathological aging. *Neuroscience & Biobehavioral Reviews* 156: 105489.
71. Behfar Q, Behfar SK, Von Reutern B, Richter N, Dronse J, Fassbender R, *et al.* (2020): Graph Theory Analysis Reveals Resting-State Compensatory Mechanisms in Healthy Aging and Prodromal Alzheimer's Disease. *Front Aging Neurosci* 12: 576627.
72. Petitet P, Spitz G, Emir UE, Johansen-Berg H, O'Shea J (2021): Age-related decline in cortical inhibitory tone strengthens motor memory. *NeuroImage* 245: 118681.
73. Bernier M, Croteau E, Castellano C-A, Cunnane SC, Whittingstall K (2017): Spatial distribution of resting-state BOLD regional homogeneity as a predictor of brain glucose uptake: A study in healthy aging. *NeuroImage* 150: 14–22.
74. Oke AF, Carver LA, Gouyon CM, Adams RN (1997): Three-dimensional mapping of norepinephrine and serotonin in human thalamus. *Brain Research* 763: 69–78.
75. Zitnik G, Chandler DJ, Waterhouse BD (2016): Norepinephrine and Synaptic Transmission in the Cerebellum. In: Gruol DL, Koibuchi N, Manto M, Molinari M, Schmahmann JD, Shen Y,

- editors. *Essentials of Cerebellum and Cerebellar Disorders*. Cham: Springer International Publishing, pp 237–241.
76. Cartford MC, Gould T, Bickford PC (2004): A Central Role for Norepinephrine in the Modulation of Cerebellar Learning Tasks. *Behavioral and Cognitive Neuroscience Reviews* 3: 131–138.
77. Bickford P (1995): Aging and Motor Learning: A Possible Role for Norepinephrine in Cerebellar Plasticity. *Reviews in the Neurosciences* 6. <https://doi.org/10.1515/REVNEURO.1995.6.1.35>
78. Mather M (2021): Noradrenaline in the aging brain: Promoting cognitive reserve or accelerating Alzheimer's disease? *Seminars in Cell & Developmental Biology* 116: 108–124.
79. Lee J, Kim H-J (2022): Normal Aging Induces Changes in the Brain and Neurodegeneration Progress: Review of the Structural, Biochemical, Metabolic, Cellular, and Molecular Changes. *Front Aging Neurosci* 14: 931536.
80. Guedj C, Monfardini E, Reynaud AJ, Farnè A, Meunier M, Hadj-Bouziane F (2016): Boosting Norepinephrine Transmission Triggers Flexible Reconfiguration of Brain Networks at Rest. *Cereb Cortex* cercor; bhw262v1.
81. Chételat G, La Joie R, Villain N, Perrotin A, De La Sayette V, Eustache F, Vandenberghe R (2013): Amyloid imaging in cognitively normal individuals, at-risk populations and preclinical Alzheimer's disease. *NeuroImage: Clinical* 2: 356–365.
82. Markesberry WR, Jicha GA, Liu H, Schmitt FA (2009): Lewy Body Pathology in Normal Elderly Subjects. *J Neuropathol Exp Neurol* 68: 816–822.
83. Błaszczyk JW (2016): Parkinson's Disease and Neurodegeneration: GABA-Collapse Hypothesis. *Front Neurosci* 10. <https://doi.org/10.3389/fnins.2016.00269>
84. Kaur R, Mehan S, Singh S (2019): Understanding multifactorial architecture of Parkinson's disease: pathophysiology to management. *Neurol Sci* 40: 13–23.
85. Wang J, Wang F, Mai D, Qu S (2020): Molecular Mechanisms of Glutamate Toxicity in Parkinson's Disease. *Front Neurosci* 14: 585584.

86. Firbank MJ, Parikh J, Murphy N, Killen A, Allan CL, Collerton D, *et al.* (2018): Reduced occipital GABA in Parkinson disease with visual hallucinations. *Neurology* 91: https://doi.org/10.1212/WNL.0000000000006007
87. Van Nuland AJM, Den Ouden HEM, Zach H, Dirkx MFM, Van Asten JJA, Scheenen TWJ, *et al.* (2020): GABAergic changes in the thalamocortical circuit in Parkinson's disease. *Human Brain Mapping* 41: 1017–1029.
88. O'Gorman Tuura RL, Baumann CR, Baumann-Vogel H (2018): Beyond Dopamine: GABA, Glutamate, and the Axial Symptoms of Parkinson Disease. *Front Neurol* 9: 806.
89. Arias de la Torre J, Vilagut G, Ronaldson A, Dregan A, Ricci-Cabello I, Hatch SL, *et al.* (2021): Prevalence and age patterns of depression in the United Kingdom. A population-based study. *Journal of Affective Disorders* 279: 164–172.
90. Movement Disorder Society Task Force on Rating Scales for Parkinson's Disease (2003): The Unified Parkinson's Disease Rating Scale (UPDRS): Status and recommendations. *Movement Disorders* 18: 738–750.
91. Goetz CG, Poewe W, Rascol O, Sampaio C, Stebbins GT, Counsell C, *et al.* (2004): Movement Disorder Society Task Force report on the Hoehn and Yahr staging scale: Status and recommendations. The Movement Disorder Society Task Force on rating scales for Parkinson's disease. *Movement Disorders* 19: 1020–1028.
92. Fry A, Littlejohns TJ, Sudlow C, Doherty N, Adamska L, Sprosen T, *et al.* (2017): Comparison of Sociodemographic and Health-Related Characteristics of UK Biobank Participants With Those of the General Population. *American Journal of Epidemiology* 186: 1026–1034.
93. Cermakova P, Formanek T, Kagstrom A, Winkler P (2018): Socioeconomic position in childhood and cognitive aging in Europe. *Neurology* 91: https://doi.org/10.1212/WNL.0000000000006390
94. Tari B, Künzi M, Pflanz CP, Raymont V, Bauermeister S (2023): Education is power: preserving cognition in the UK biobank. *Front Public Health* 11: 1244306.

95. Nikhra V (2017): The Aging Brain: Recent Research and Concepts. *GGS* 1.

<https://doi.org/10.31031/GGS.2017.01.000511>

Figure legends:

Figure 1: Methodological overview. We derived voxel-wise maps of fALFF, LCOR, and GCOR from individual rs-fMRI data (**A**). First, this data was used to explore group-level voxel-wise aging changes in fALFF, LCOR and GCOR in the healthy cohort ($n_{HC}=25917$, **A**, right column). Second, we used PET maps of 19 neurotransmitter systems (**B**) to calculate the spatial correlation (co-localization) with both, the group-level aging effects (**C**) and individual fALFF, LCOR, and GCOR (**D**). We Fisher (z-)transformed the Spearman correlation coefficients ρ to ensure a normal distribution and examined the effects of age on the co-localization data of the healthy cohort (**E**). The blue cloud illustrates co-localization strengths (kernel density estimation of all transformed Spearman correlation coefficients) of the healthy cohort. For each pair of measure and neurotransmitter map, we analyzed mean co-localizations (yellow), linear aging effects (green), as well as differences in variances across subjects in the youngest (44–60 years) and oldest (68–82 years) third ($n_{Both}=8\,639$; red). Vertical dashed red lines were added for illustration only and do not correspond to the actual variance of the respective subpopulation. Afterwards, we normatively modeled the co-localization strengths depending on age and sex (**F**, left) in order to calculate the deviation in subjects with manifest Parkinson’s disease ($n_{PD}=58$; crosses). Here, we show the predicted means (solid lines) and 25% and 75% percentile (dashed lines) derived from the normative model for both men (blue) and women (orange). We analyzed whether the deviation (z-)scores of subjects with Parkinson’s disease were significantly different from a null distribution (**F**, box plot). In this example, the distribution was significantly below a null distribution, indicating that patients with PD exhibit lower Spearman correlation coefficients than the norm. Last, we quantified the mean regional contribution to the observed deviation score across subjects with Parkinson’s disease (**G**, left), as well as the functional differences in patients with Parkinson’s disease compared to an age- and sex-matched subcohort of healthy controls ($n_{HC\text{matched}}=17,900$; **G**, right). The functional differences were quantified by calculating the regional effect sizes (Cohen’s d).

Figure 2: Group-level voxel-wise aging effects in each functional measure and associations with neurotransmitter systems.

A: Colors in the voxel-wise plots of thresholded group-level aging effects indicate annual decrease (blue) or increase (red) in fALFF (top), LCOR (middle), and GCOR (bottom). **B, left column:** Significant ($P_{FDR} < 0.05$) linear correlations between annual rate in brain functional measure and neurotransmission. Vertical black lines indicate the uncertainty of Fisher's z-transformed Spearman correlation coefficient estimated according to Bonett & Wright(63). **B, right column:** Exemplary scatter plots show how the annual change in fALFF, LCOR, or GCOR spatially correlate with the PET signal of specific neurotransmitter systems. Colors group receptors and transporters of the same neurotransmitter system, i.e., serotonin (red), dopamine (blue), acetylcholine (green), glutamate (pink) and GABA (purple), cannabinoid (mint), opioid (yellow), norepinephrine (orange), and histamine (turquoise).

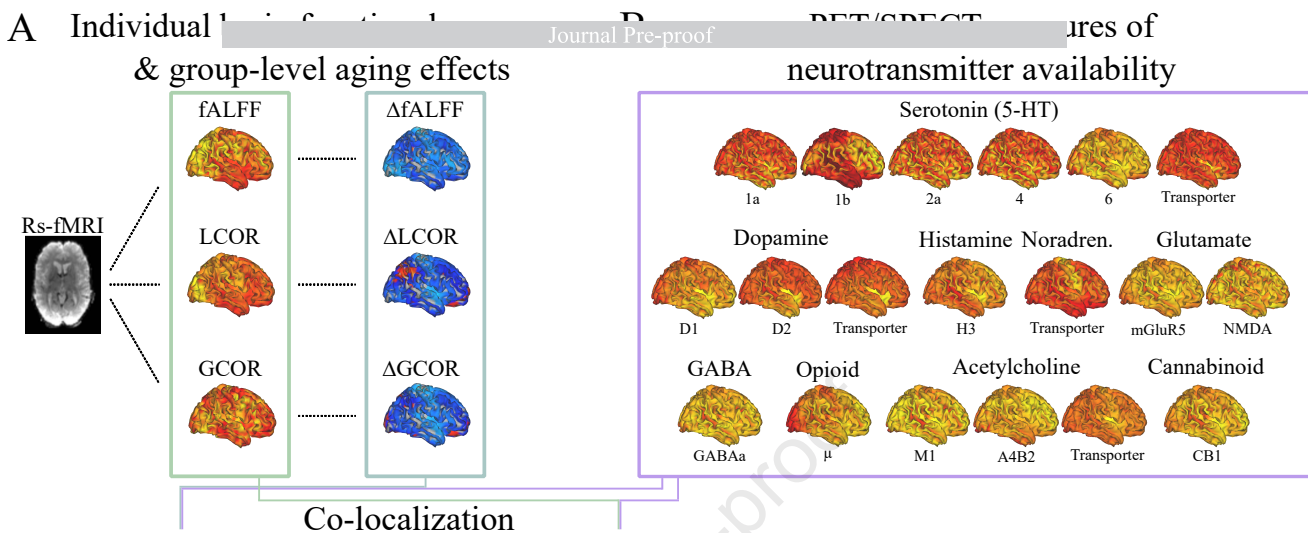
Figure 3: Single-subject co-localizations between brain functional measure and neurotransmitter systems depend on age. **A, left column:** Overview about all significant linear aging effects ($P_{\text{Bonferroni-Holm}} < 0.05$) in the co-localization strengths (Fisher's z-transformed Spearman correlation coefficients) between each pair of brain functional measure (fALFF, LCOR, GCOR) and neurotransmitter system. Error bars correspond to the standard error of parameter (slope) estimation. **A, right column:** Exemplary plots show how co-localization strengths between brain functional measures (fALFF: top, LCOR: middle, GCOR: bottom) and specific neurotransmitter systems depend on age. The black, horizontal line indicate the population mean co-localization (cf. Supplementary Figure 6 for an overview about all co-localization means). The colored clouds show the kernel density estimation of Fisher's z-transformed Spearman correlation coefficients of the healthy cohort. The slope of the colored line (linear fits) corresponds to the bar plots in the left column. **B, left column:** Each plot shows the effect size (F-statistic) of mean squared error (MSE) differences between younger and older adults. We show bar plots regarding neurotransmitter systems whose co-localization with the respective brain functional measure was previously shown to be significantly non-constant (White-test, $P_{\text{FDR}} < 0.05$). All pairs of brain function and PET map whose co-localization variance was significantly ($P_{\text{FDR}} < 0.05$) different between the older and the younger subpopulations are highlighted by asterisks (*: $P_{\text{FDR}} < 0.05$; **: $P_{\text{FDR}} < 0.01$; ***: $P_{\text{FDR}} < 0.001$). F-statistics (MSE of older divided by MSE of younger adults) above 1 correspond to a larger variance in the older subpopulation. **B, right column:** Exemplary plots visualize the individual squared errors of the co-localizations between younger and older adults. Box plots visualize both distributions. Note, that per definition, the squared errors are positive. Due to the kernel density estimation of all squared errors the colored clouds exceed the null level. Colors group receptors and transporters of the same neurotransmitter system according to the same scheme as described in Figure 2.

Figure 4: Subjects with PD deviate from normative models of co-localization between brain function and neurotransmitter systems. **A:** The purple cloud shows the kernel-density-plot of Fisher's z-transformed Spearman correlation coefficients of the healthy cohort regarding the spatial correlation of LCOR and GABAa. Solid and dashed lines show the predicted mean and predicted 25% or 75% percentile of men (turquoise) and women (orange) derived from the normative models. Crosses indicate the co-localization levels of patients with PD. **B:** Box plot showing the significant deviation from the norm (null) in patients with PD. **C:** Deviation scores in PD are significantly correlated with disease duration. **D–F:** Box plots showing the deviation scores that were significantly different from the norm (null) regarding fALFF (**D**), LCOR (**E**), and GCOR (**F**). *, **, and *** indicate Bonferroni-Holm corrected significant deviations of the distributions from a null distribution with exact $P<0.05$, $P<0.01$, and $P<0.001$. Colors in box plots group receptors and transporters of the same neurotransmitter system according to the same scheme as described in Figure 2. **G–H:** Significant ($P_{\text{FDR}}<0.05$) regional differences (effect sizes, Cohen's d) between PD and the matched subgroup of healthy controls in LCOR (**G**) and GCOR (**H**). Lower values in PD are indicated by blue areas. Effect sizes of all region are provided in Supplementary Figures 17–19.

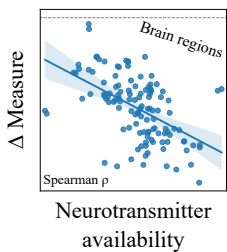
Tables:

	Healthy controls (HC)	Females (HC)	Males (HC)	Manifest Parkinson's disease (PD)	HC matched to PD
Sample Size	25917	14000	11917	58	17400
Age [yr]	64.03 ± 7.5	63.5 ± 7.4	64.7 ± 7.6	68.6 ± 6.5	67.6 ± 6.0
Age Statistics	-	T=-12.48; P<0.0001; Cohen's d=-0.16		T(57.32)=1.15; P=0.26	
Sex, Male	11917 (46%)	-	-	32 (55.2%)	8988 (51.7%)
Sex Statistics	-	-	-	$\chi^2(1)=0.29, P=0.59$	
TIV [L]	1.548 ± 0.152	1.467 ± 0.116	1.643 ± 0.133	-	-
TIV Statistics	-	T=-113.0; P<0.0001; Cohen's d=-1.42	-	-	-

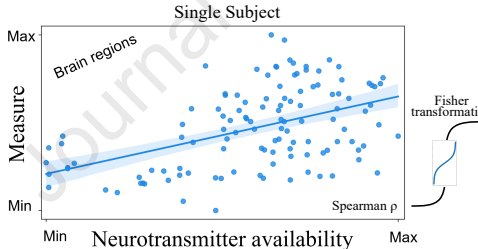
Table 1: Demographical characteristics. Normative modeling of co-localizations between brain function and neurotransmitter systems is based on the data of healthy controls. Regional differences in brain measures in patients with PD were calculated with respect to an age- and sex-matched subcohort of healthy controls.



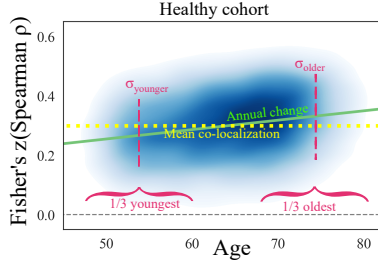
C Group-level aging effects



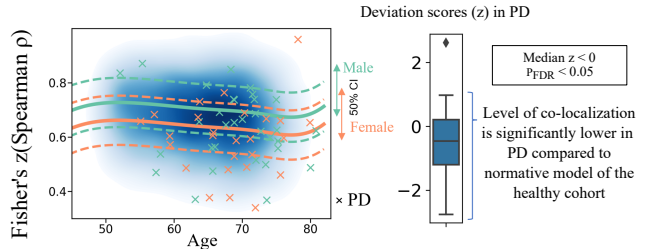
D Individual measures of brain function



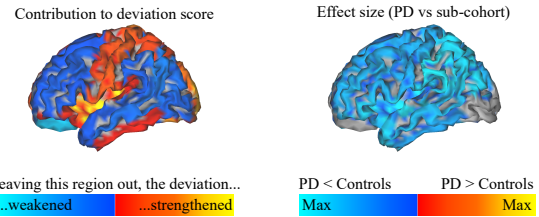
E Aging effects across individual co-localizations



F Normative modeling & deviation in Parkinson's disease

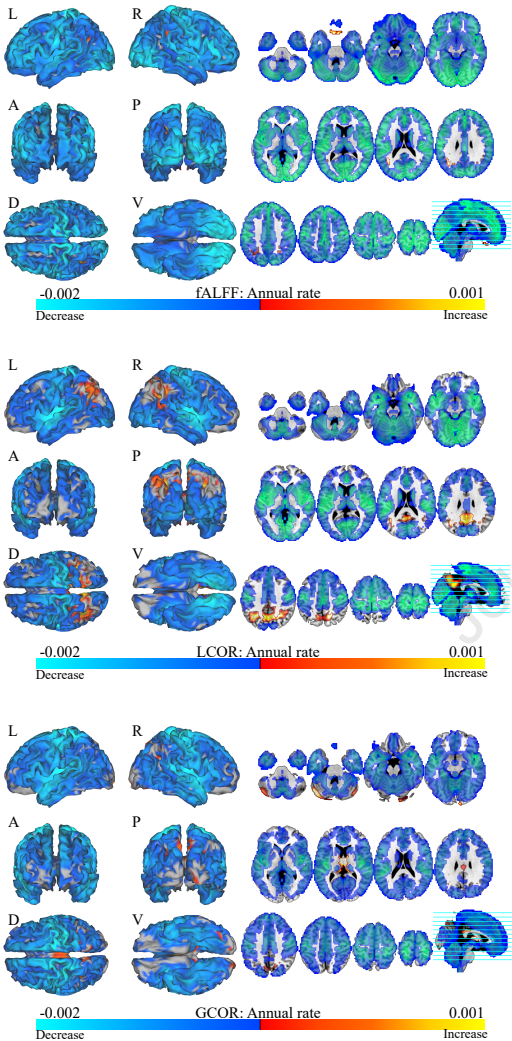


G Regional contribution & differences between Parkinson's disease and control cohort

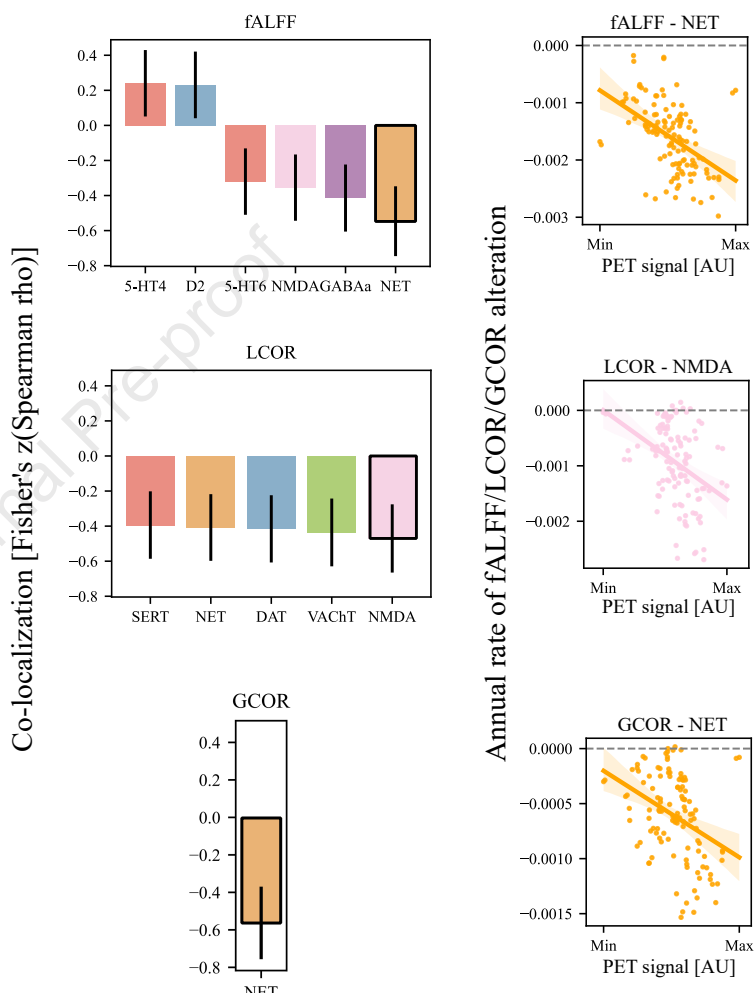


A

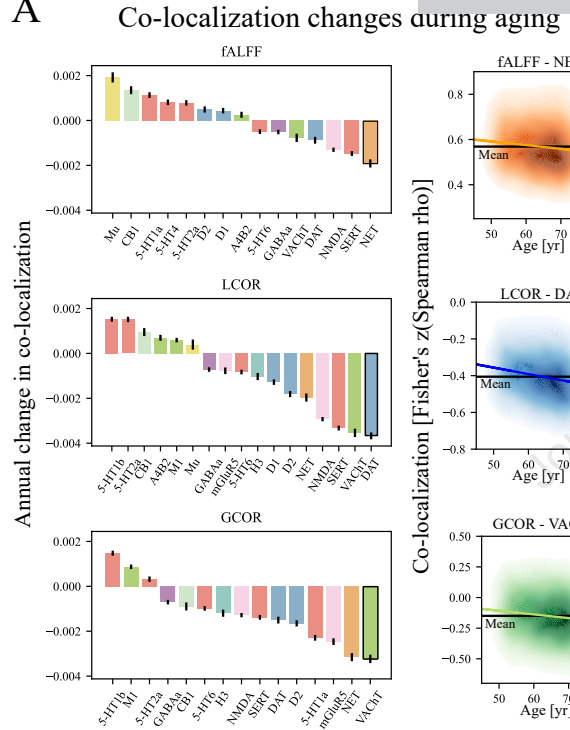
Voxel-wise aging

**B**

Journal Pre-proof Aging and neurodegeneration with neurotransmission



A



Journal Pre-proof

B

